Chapter 3

Bio-inspired Design and Fabrication of Super-Strong and Multifunctional Carbon Nanotube Composites

Xiaohua Zhang, Xueping Yu, Jingna Zhao and Qingwen Li

Additional information is available at the end of the chapter

http://dx.doi.org/10.5772/62810

Abstract

Carbon nanotubes (CNTs) are ideal scaffolds to design and architect high-performance composites at high CNT volume fractions. In these composites, the CNT alignment determines the level of aggregation and the structure morphology, and thus the load transfer efficiency between neighboring CNTs. Here, we discuss two major solutions to produce high-volume fraction CNT composites, namely the layer-by-layer stacking of aligned CNT sheets and the stretching of entangled CNT webs (networks). As inspired by the growth procedure of natural composites, the aggregation of CNTs can be well controlled during the assembling process. As a result, the CNTs can be highly packed, aligned, and importantly unaggregated, with the impregnated polymers acting as interfacial adhesion or mortars to build up the composite structure. The CNT/bismaleimide composites can yield a super-high tensile strength up to 6.27–6.94 GPa and a modulus up to 315 GPa.

Keywords: carbon nanotube composite, high volume fraction, super-strong, multifunctionality, bio-inspired

1. Introduction

Since their discovery in 1991 [1], carbon nanotubes (CNTs) have generated huge activity in most areas of science and engineering due to their unprecedented mechanical, electrical, and thermal properties. For example, lightweight multifunctional composites with enhanced properties can be produced by effectively incorporating individual CNTs into polymer matrices [2, 3]. The first polymer nanocomposites using CNTs as a filler were reported in 1994, where the CNTs were

aligned within the epoxy matrix by the shear forces induced by cutting with a diamond knife [4]. In the following decades, tremendous research has been done to develop CNT-reinforced composites with a high strength and modulus. However, as compared to individual CNTs, the composites produced by these "conventional" fabrication methods usually do not exhibit significantly improved mechanical and electrical performances. This is mainly due to the limited content of CNT (usually under 5 wt%). Furthermore, it is also important to introduce a uniform CNT dispersion in polymer matrix and adhesion between different constituents in improving the composite performances.

Recently, a new type of CNT composite material has been developed using macroscopic CNT assemblies as raw materials, namely high-volume fraction CNT composites, where the volume fraction of CNT is usually much larger than 50%. To obtain these composites, the macroscopic forms of entangled or aligned CNTs, that is, fibers [5–7], forests [8–12], and membranes [13–16] are used as scaffolds, and the polymer is impregnated into the free pores of these CNT network. Of great importance, the super-aligned CNT sheets drawn out from spinnable CNT forests [17] and the entangled CNT webs (networks) grown with an injection chemical vapor deposition method [18] have superb advantages in obtaining super-strong high-volume fraction CNT composites.

Furthermore, to design the structure for high-performance composites at high CNT fractions, nature can offer us with scientific and technological clues from the formation process of biological composites. The natural composite materials are usually built up by common organic components via the naturally mild approaches [19], such as super-tough spider fibers [20], strong hard nut skins [21], and wear-resistant molluscan shells [22]. In these composites, the major components such as proteins, cellulose molecules, and nanometer-sized crystals of carbonated calcium phosphates or calcium carbonates are homogeneously distributed and orientated along with other co-existing components [20, 23]. This provides us new approaches to obtain super-strong CNT composites [24]. For CNT composites, due to the strong tendency to agglomerate between CNTs [25–29], it is still difficult to uniformly disperse CNTs within polymer matrix at a high-volume fraction and thus to mimic the natural composites. Fortunately, CNTs can be treated as linear macromolecules, and thus, the processing on them can be dealt with in a biomimic way. Therefore, it becomes possible to mimic the formation process of biological composites to design new type of CNT composites.

This chapter thus aims at the structural design of super-strong and multifunctional CNT composites at high-volume fractions. Various processing methods are presented in the following sections, namely the layer-by-layer stacking of aligned CNT sheets, stretching on entangled CNT webs, and, most importantly, bio-inspired aggregation control to optimize the composite structure.

2. Conventional composite processing

Solution processing and melt processing have been widely used to prepare composites, where CNTs and polymer matrix can be well mixed together. For the solution treatment, CNT and polymer are mixed in a suitable solvent before evaporating the solvent to form a composite

http://dx.doi.org/10.5772/62810

film. One benefit of such method is that agitation of the CNT powder in a solvent facilitates CNT de-aggregation and dispersion. In general, agitation of CNT or of CNT/polymer mixture is provided by magnetic stirring, shear mixing, reflux, and, as widely used, ultrasonication.

In an early study [30], multiwalled CNTs were dispersed in chloroform by sonication. Then, polyhydroxyaminoether (PHAE) was dissolved in the CNT/chloroform dispersion and mixed by additional sonication. The suspension was poured into a Teflon mould and dried in ambient conditions to obtain the CNT composites. In the following decade, various similar methods have been reported. For example, CNTs were first chemically modified and then dispersed in water [31]. The dispersion was blended with poly(vinyl alcohol) (PVA)/water solution to give composite solutions which were used to prepare the composites.

As pristine CNTs cannot be well-dispersed in most solvents, surfactants such as sodium dodecyl sulfate (SDS), sodium dodecyl sulfonate (SDSA), polyvinylpyrrolidone (PVP), and dodecyl tri-methyl ammonium bromide (DTAB) were also used to assist the CNT dispersion before mixing with the polymer solution [32–38]. This technique results in excellent dispersion with no derogatory effects on film properties observed. However, the existence of surfactant could affect the interfacial strength between CNT and polymer.

For those polymers which are insoluble in the designed solvent, melt processing has become a common alternative. For example, amorphous polymers can be processed above their glass transition temperature, and semi-crystalline polymers can be heated above the melt temperature to induce sufficient softening [39–43]. In general, melt processing involves the melting of polymer pellets to form a viscous liquid. CNTs can be mixed into the melt by shear mixing. Bulk samples can then be fabricated by techniques such as compression molding, injection molding, or extrusion. In such approach, the optimized processing conditions depend on not only the types of CNT, but also the whole range of polymer–nanotube combinations. This is because nanotubes can effect melt properties such as viscosity, resulting in unexpected polymer degradation under conditions of high shear rates [39].

The dispersion and melting treatments have been widely used to obtain the composite structure by well mixing polymer and CNTs. Besides the structure design, interfacial covalent bonding is often applied in these methods in order to increase the composite performances. For example, in situ polymerization enables grafting of polymer molecules onto the wall of CNT and thus allows the preparation of composites with high nanotube loading. It is also particularly important for the preparation of insoluble and thermally unstable polymers, which cannot be processed by solution or melt processing. For example, due to their π-bonds, CNTs can participate in the polymerization of poly(methyl methacrylate) (PMMA), which resulted in a strong interface between the CNT and the PMMA matrix [44–46]. Poly(p-phenylene benzobisoxazole) (PBO)/CNT composites were also obtained with in situ polymerization by introducing CNTs in poly(phosphoric acid) (PPA) [47]. For CNT composites using polyamide, in situ polymerization can be realized between carboxylated CNTs and ε-caprolactam monomer [48].

In situ polymerization has been applied for the preparation of composites with CNT and various types of polymer. In this approach, covalent functionalization of CNT surface plays a

special role for CNT processing and applications [49–55]. "Grafting from" and "grafting to" are the two main strategies to introduce covalent bonding between polymers and CNTs [2]. In the former approach, the initiators are immobilized onto CNT surfaces and then, the monomers are in situ polymerized with the formation of covalent bonding between polymer and CNT. The latter approach is based on attachment of already preformed end-functionalized polymer molecules to functional groups on CNT surface via different chemical reactions. There have been many reports on the grafting techniques, where the grafted polymers include PMMA [56–60], polyethylene (PE) [61–64], polystyrene [65–67], chitosan [68, 69], and so on.

There have been tremendous development on CNT composites using these conventional processing methods over the past 20 years. However, the dispersion of long CNTs is still hindered by their entanglement and aggregation, and the CNTs are limited to a low fraction and randomly orientated. Consequently, the final composite strength is usually below 400 MPa [70, 71]. Further, in situ polymerization or hot stretching is also not very effective in improving the mechanical properties [2, 28, 72]. Therefore, further development is still of great necessity, especially on the design of composite structure.

3. Layer-by-layer stacking of aligned CNTs

The large mass scale production of CNT has pushed the rapid development of CNT in various applications [73, 74]. However, the random orientation and entanglement hinder the structure design of high-volume fraction and aligned CNT composites. The development on spinnable CNT forests opened a new way towards such composite structure. CNT forests (also called CNT carpets) superficially resemble bamboo forests, except that the CNT "trees" in these forests can be over 50,000 times longer than their diameter, and this very high aspect ratio is useful for optimizing the mechanical and electrical properties. As a unique type of CNT forests, known as spinnable forests, one can continuously transform the vertically aligned CNTs into a horizontally aligned CNT sheet by a simple dry drawing or spinning method [17, 75–79]. Thus, the spinnability (or processability/drawability) is defined by the stable width and continuous length of the spun-out CNT sheets and the available spinning rates [80].

3.1. CNT/polymer composite films

The spinnable CNT forests have been successfully used to fabricate high-performance composite films. At first, the spun-out aligned CNTs were stacked together at different orientations to make a CNT preform [81]. After a resin transfer molding process, homogeneously dispersed CNT/epoxy composites with a CNT loading up to 16.5 wt% were obtained. The Young's modulus and tensile strength of the composites reached 20.4 and 231.5 MPa, corresponding to 716 and 160% improvement compared to pure epoxy.

To further improve the CNT volume fraction, the CNT sheets were stacked in a continuous winding way with the aid of solution spraying [12]. **Figure 1A** shows the schematic of spray winding, where a CNT sheet is continuously wound onto a rotating mandrel on which micrometer-sized polymer solutions are deposited. With the long-chain polymer PVA, the aligned composite film exhibited a tensile strength up to 1.8 GPa at a CNT content of 65 wt%

http://dx.doi.org/10.5772/62810

[12]. Due to the alignment, the composite film was also stiff (modulus of 40–96 GPa), tough (energy absorbed before fracturing of 38–100 J g^{-1}), and electrically conductive (conductivity of 780 S cm^{-1}). By following this method, high-performance CNT composites with epoxy, polyimide (PI), and bismaleimide (BMI) were produced [82–85].

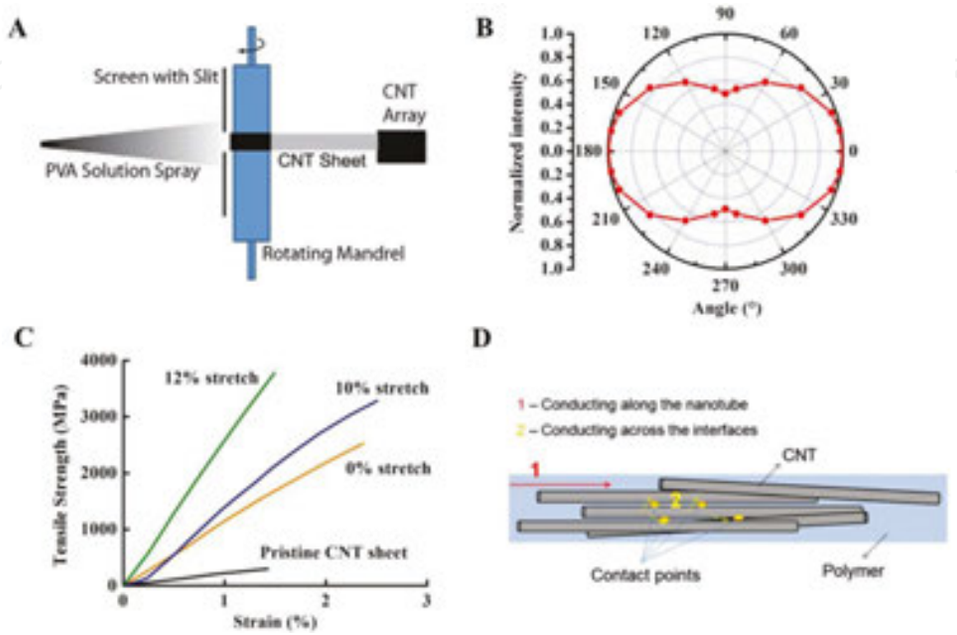

Figure 1. (A) Schematic view of spray winding. A CNT sheet is drawn out from a spinnable forest and continuously wound onto a rotating mandrel on which micrometer-sized droplets of polymer solution are deposited [12]. (B) Normalized intensity of G′-band peak as a function of the angle between the sample's longitudinal direction and the polarization axis of the incident laser beam. (C) Typical stress–strain curves of pristine CNT sheet, unstretched and stretched composites, demonstrating a significant improvement on mechanical properties through aligning and straightening of CNTs [82]. (D) Schematic presentation of heat conduction mechanism in high-volume fraction CNT composites [83].

The layer-by-layer stacking allowed a high level of CNT alignment in the final composites. The alignment can be quantitatively measured with polarized Raman spectroscopy [8, 86]. **Figure 1B** shows the normalized intensity of Raman G′-band peak as a function of the angle between the sample's longitudinal direction and the polarization axis of the incident laser beam; according to the results, we have reported previously [12]. The normalized G′ peak was strongest at 0° (along the CNT orientation) and monotonically decreased from 1 to 0.493 at 90° (perpendicular to the orientation).

To further improve the CNT alignment, a pair of stationary rods was placed between the CNT forest and the rotating mandrel. Due to the surface friction, the rods induced a certain shear stretching on the CNT sheet [82]. As a result, the mechanical, thermal, and electrical properties of the composites were simultaneously improved; the film exhibited a strength of 3.8 GPa, Young's modulus of 293 GPa, electrical conductivity of 1230 S cm^{-1}, and thermal conductivity of 41 Wm^{-1} K^{-1}. **Figure 1C** shows the stress–strain curves of pristine CNT sheet without matrix and CNT composite sheets stretched to various stretch ratios, where the effect of CNT alignment and straightness can be clearly seen.

In these composite films, the longer the CNTs the higher the thermal and electrical conductivities are. However, the mechanical properties including the strength and modulus exhibited no CNT length dependency [83]. (A) Setup for layer-by-layer stacking of aligned CNT sheets. (B) As-prepared CNT film on a mandrel. (C) Flexible CNT film strip. (D,E) Photographs of a shining CNT strip and a strip coated with a 12 nm gold layer. Inset in (D) is the shape of a water droplet on the strip. (F) SEM image of a woven fabric consisting of CNT strips. **Figure 1D** shows a schematic of thermal (electrical) conducting mechanism for the high-volume fraction CNT composites. Due to the long tube length, thermal conduction across the interfaces is as not dominant as that along the CNTs. On the contrary, the thermally insulating polymer restricts the phonon mobility at the interface in short-CNT-reinforced composites. This means that the high interfacial thermal resistance can strongly limit the total thermal conductivity. However, with increasing the tube length, several issues might affect the mechanical performance. First, the average tube diameter and wall number increased with the tube length, leaving the aspect ratio remaining nearly unchanged. Second, the increased tube length usually causes more aggregation between the CNTs. These two issues both hinder the efficiency of interfacial stress transfer.

3.2. Super-strong CNT assembly film

As inspired by the forest-based fiber spinning where macroscopic one-dimensional assembly fiber with pure (neat) CNTs can be produced [75, 76], the layer-by-layer stacking can be also used to fabricate pure CNT films with high mechanical performances. Although no polymer molecules are impregnated, various solvents such as ethanol, acetone, and *N*,*N*-dimethylmethanamide (DMF) are used to densify the CNTs. The solvent can be either sprayed onto the mandrel during the winding process or dip onto the CNT film after the winding [87]. **Figure 2**

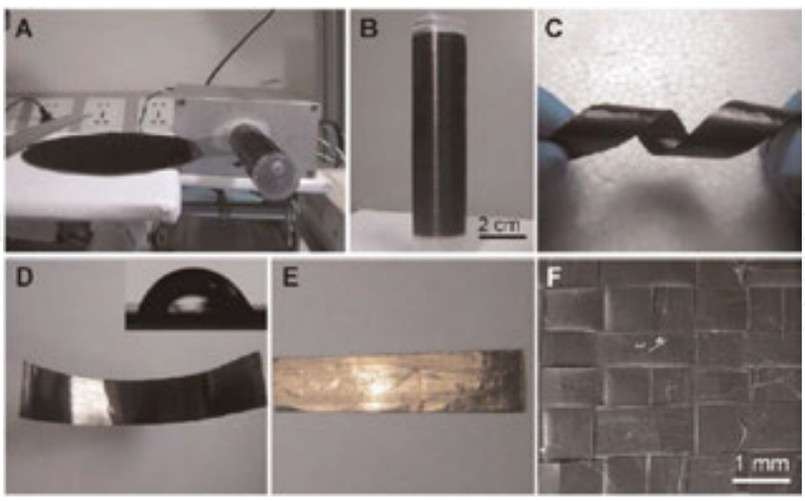

Figure 2. Pure CNT assembly films can be produced by layer-by-layer stacking of as-drawn CNT sheets with the aid of solvent densification [87] (A) Setup for layer-by-layer stacking of aligned CNT sheets. (B) As-prepared CNT film on a mandrel. (C) Flexible CNT film strip. (D,E) Photographs of a shining CNT strip and a strip coated with a 12 nm gold layer. Inset in (D) is the shape of a water droplet on the strip. (F) SEM image of a woven fabric consisting of CNT strips.

http://dx.doi.org/10.5772/62810

shows the CNT films obtained using 2–3-walled 4–6-nm-diameter CNTs. The CNT film had a smooth and shinning surface, was flexible, and exhibited tensile strengths of 1.1–1.9 GPa and Young's modulus of 40–90 GPa. Obviously, the alignment allowed a high degree of utilization of the intrinsic properties of CNT.

The CNT alignment was further improved when a stretch-dip-drying approach [88] was applied to the as-spun CNT films (**Figure 3A**). After such treatment, the CNT film was observed to significantly shrink in width by 22–39%, corresponding to an increased packing density. As compared to the simple solvent densification, the mass density of the film increased from 0.5–0.85 to 1.21–1.35 g cm^{-1}. Therefore, with the improved CNT alignment, the obtained CNT films exhibited significantly improved strength, up to 2.58–3.19 GPa.

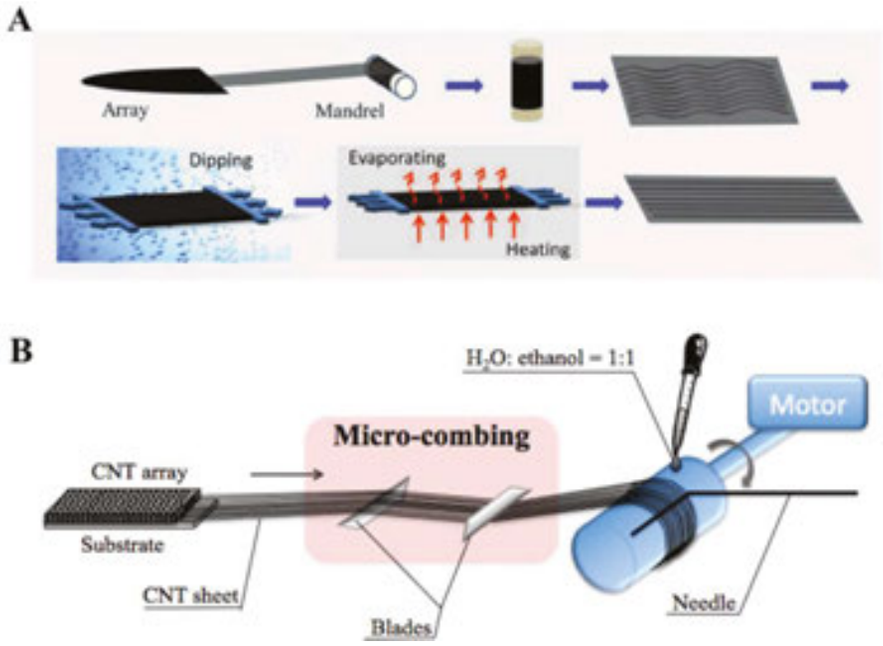

Figure 3. Two solutions to further improve the CNT alignment. (A) CNT alignment can be remarkably improved by the stretch-dip-drying method [88]. (B) Schematic view of the microcombing process which can mitigate the CNT waviness [89].

In another study, the as-drawn CNT sheets were "combed" to become straighter and aligned before being layer-by-layer stacked [89]. **Figure 3B** shows the schematic view of such microcombing. As the microcombing mitigates the CNT waviness and thus reduces the sheet defects, the final CNT film exhibited very high Young's modulus of 172 GPa and the similar tensile strength of 3.2 GPa. Surprisingly, the electrical conductivity was as high as 1800 S cm^{-1}, higher than other CNT films fabricated using the aligned CNT sheets.

All these studies show clearly that the CNT alignment plays the most important role in determining the mechanical and electrical properties. Nevertheless, solvents still have interesting influences on the microstructure of aggregated CNTs. For example, the acetone-densified pure CNT films usually had a higher strain at break than the ethanol-densified CNT films [89]. Such phenomenon is due to the different volatility of solvent [90]. When a high-

volatile solvent was used, the CNT films exhibited a certain level of networking, which can absorb additional energy during the tensile stretching. As a result, the film's plasticity and toughness can be improved. This means that, even for the aligned CNT films, it is still possible to tune the internal microstructure of the highly packed CNTs, and thus to influence the film's mechanical and electrical properties.

4. Stretching on entangled CNT webs

As the CNT length can only reach several hundred micrometers for the forest-based spinning, the aspect ratio of the CNTs is thus limited to be in the range of 10^4. On solution to increase the aspect ratio is the decrease in diameter, like the spinnable few-walled CNT forests [87, 91]. A different way is to grow super-long CNTs, up to millimeter-long. For example, the millimeter-long and small-diameter (~3–8 nm) 2–5-walled CNTs provided a aspect ratio up to 10^5 [92]. These CNTs substantially entangled with each other due to the floating catalyst synthesis and aero-gel condense method [18]. The films with entangled CNTs (CNT webs) can reach up to a meter long and are commercially available, which makes them practical for manufacturing bulk composites [93].

4.1. Direct stretching

A simple mechanical-stretch method can be used to align the CNTs in the entangled webs [93]. For example, for a 40%-stretched CNT film (i.e., the post-stretch film was 40% longer than the pre-stretch one), the degree of CNT alignment can be dramatically improved (**Figure 4A**). Polarized Raman scattering tests were conducted to calculate the alignment degree [94]. From the trend of the best fitting, it was predicted that the near-perfect alignment (more than 95% CNTs aligned along stretch direction) at an approximate 50% stretch ratio [93]. This means that it is still necessary to further improve the plasticity of the CNT webs.

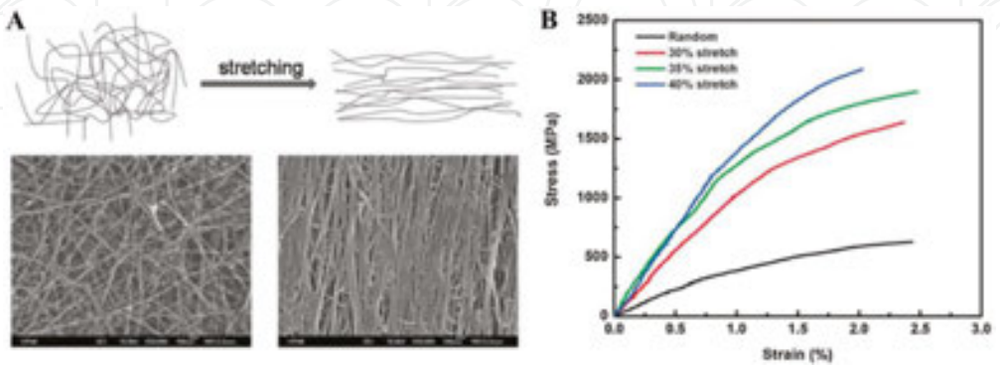

Figure 4. Direct stretching on entangled CNT webs resulted in the remarkably improved mechanical performances [93]. (A) Schematic illustration of mechanical stretching to align CNTs in the entangled webs. (B) Typical tensile stress–strain curves of produced CNT/BMI composites at different stretch ratios.

http://dx.doi.org/10.5772/62810

The mechanical properties of the pure CNT webs were improved with the stretch ratio. The film's tensile strength and Young's modulus were just about 205 MPa and 1.10 GPa for the unstretched films. After the stretching, the CNT packing density also increased with the alignment. For the 30, 35, and 40% stretch ratios, the strength increased up to 390, 508, and 668 MPa, respectively, and the modulus along the alignment direction showed even more dramatic improvements, up to 11.93, 18.21, and 25.45 GPa, respectively.

When BMI was introduced into the CNT webs, either as-produced or stretched, there were further improvements on the mechanical properties. The tensile strength of the randomly dispersed CNT/BMI composite (CNT loading of about 60 wt%) was approximately 620 MPa, and the Young's modulus was 47 GPa. After stretching by 30, 35, and 40%, the strength and modulus became 1600 MPa and 122 GPa, 1800 MPa and 150 GPa, and 2088 MPa and 169 GPa, respectively (**Figure 4B**).

4.2. CNT functionalization

Although the improvement in CNT alignment benefited the mechanical properties, substantial CNT pull-outs were observed at the fracture of the composites [93], corresponding to weak interfacial bonding. To overcome this problem, a follow-up effort was performed by improving the bonding with epoxidation functionalization [95]. To realize the interfacial reaction between CNT and BMI, the stretched CNT films were placed in peroxide acid (*m*-chloroperoxybenzoic acid or *m*-CPBA)/dichloromethane solution for functionalization. The functionalized CNT films were placed in a vacuum oven at 80°C for 30 min to evaporate the residual dichloromethane. Then, the CNT films were impregnated with BMI resin solution to prepare prepregs with approximately 60 wt% CNT loading. During the curing process, the reaction between the functionalized CNTs and BMI resin formed interfacial covalent bonds, whose mechanism is proposed as shown in **Figure 5A**. First, *o*,*o*′-diallyl bisphenol A reacted with the epoxide groups of the pre-functionalized CNTs, according to the epoxy-phenol reaction mechanism [96]. Then, in ene and Diels–Alder reactions, three-dimensional cross-linked structures were formed

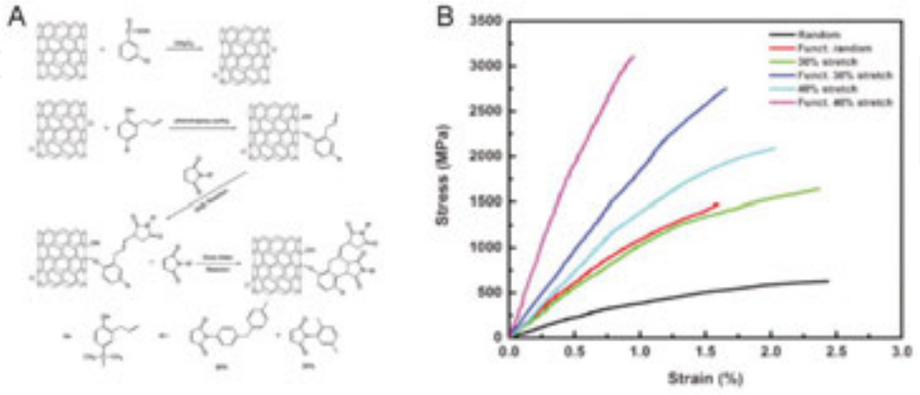

Figure 5. CNT functionalization improved the interfacial bonding strength and thus increased the tensile properties of the CNT/BMI composites [95]. (A) Proposed reaction mechanism of functionalized CNTs and BMI resin. (B) Typical tensile stress–strain curves of random and stretch-aligned CNT/BMI composites with and without functionalization.

between the derivative and the other two BMI components [97, 98]. The covalent bonding between CNT and BMI dramatically enhanced the interfacial adhesion, and thus, the improved load transfer was achieved by the functionalization.

Figure 5B shows typical stress–strain curves of CNT/BMI composite films along the CNT alignment direction. As compared to the pristine random CNT/BMI composites, the tensile strength and Young's modulus dramatically increased with the increase of alignment. After the functionalization to for interfacial covalent bonds, the mechanical properties of the resultant film were further improved. The strength and modulus of functionalized random CNT/BMI composites were 1437 MPa and 124 GPa, respectively. For the functionalized and 30%-stretched composites, the strength and modulus increased up to 2843 MPa and 198 GPa, respectively. The 40% stretch alignment together with interfacial functionalization resulted in the highest mechanical performances, where the strength and modulus were surprisingly as high as 3081 MPa and 350 GPa, respectively.

5. Bio-inspired aggregation control

The high-volume fraction CNT composites have exhibited exciting advantages in achieving high mechanical and electrical performances. However, due to the aggregation of nanometer-sized components, there is still a severe problem in paving the way to stronger materials [99]. The aggregation control is very necessary and can be demonstrated by a comparison of the structures of carbon fiber-reinforced polymer, aggregated and unaggregated CNTs in composites, as shown in **Figure 6** [24]. The large specific surface area is one important advantage of CNT. When the aggregated CNTs were used to replace solid carbon fibers, as observed in many reports [12, 82, 87, 93, 95], larger interfacial contact area was formed, and tensile strengths of the CNT composites range from 2.08 to 3.8 GPa [82, 93, 95]. However, in the aggregation phase, the load transfer is not as efficient as at the interface. Thus, such aggregation phase might become the weak parts in the composites and hinders further reinforcement. In an ideal structure, the nanometer-sized components should be uniformly distributed in the matrix

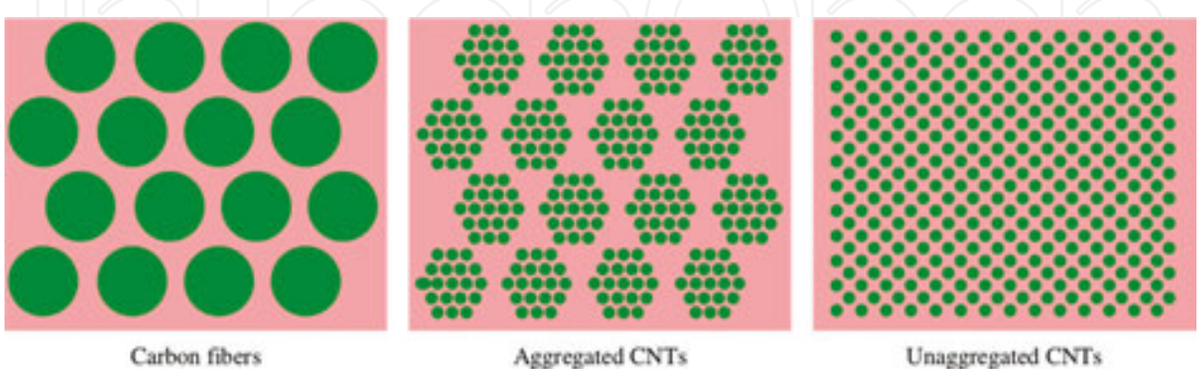

Figure 6. Schematics of carbon fiber-reinforced polymer, composite structure with aggregated CNTs, and ideal structure containing unaggregated CNTs, respectively [24].

http://dx.doi.org/10.5772/62810

without formation of any aggregation phases. Therefore, all the interfaces can play roles in shear load transfer.

The CNT aggregation arises from van der Waals (vdW) attraction and can be enhanced in wet environment. The situation becomes very severe in the layer-by-layer stacking of aligned CNT sheets with the aid of solution spray [12, 82, 87], where the CNTs (or more commonly, small-sized CNT bundles) usually aggregate first into large-sized bundles and then are surrounded by polymer matrix. **Figure 7A** and **B** show the aggregation phase of CNT, which were results of the layer-by-layer stacked aligned CNTs and the highly stretched CNT webs, respectively. Usually, the CNT aggregation was observed in a scale of hundreds of nanometer. Nevertheless, due to the entanglement, the preformed CNT webs were found to be more optimal than the forest-based CNT sheets in realizing the aggregation control.

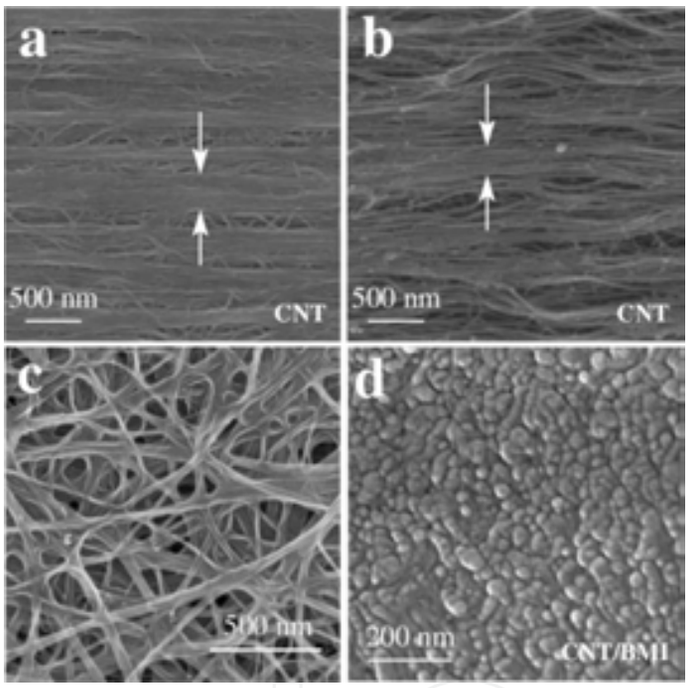

Figure 7. SEM characterization of different CNT assembly structures [24]. (A) CNT aggregation in the layer-by-layer stacking of as-spun aligned CNT sheets. (B) CNT aggregation in the stretched dry films composed by entangled CNTs. (C) Acetone-densified CNT webs maintained the feature of entanglement. (D) Cross section of the optimal CNT/BMI composite structure using focused ion beam treatment, where the aggregation level of CNTs was limited within a dimension of 20–50 nm.

5.1. Impregnation without introducing aggregation

As-inspired by the natural composite structures, the entanglement was utilized to produce the optimal composite structure where the CNTs and polymer matrix co-existed and uniformly distributed among each other. This is because that the CNT webs can maintain the CNT entanglement after liquid densification. For example, after being densified with acetone, the pore sizes of the CNT webs decreased from >500 nm to ~100–200 nm, while the CNTs were still unaggregated and randomly distributed (**Figure 7C**). This is reminiscent of the formation

process of biological composites. During the formation, the matrix and the major components are simultaneously grown from stem cells at the optimized fractions to maximize the interfacial stress transfer. Therefore, we should introduce the polymer matrix into the CNT network prior to any other treatments, just to "grow" an initial composite configuration without CNT aggregations. Here, the BMI resins were dissolved in acetone and impregnated into the CNT webs. After the stretching, densification, and thermal curing, the CNTs were still found to be unaggregated (at least no larger than 50–100 nm), as shown in **Figure 7D**.

5.2. Multi-step stretching processes

The entangled CNTs can be re-assembled and aligned by a high level of stretching. This requires the CNT film to possess high plasticity. The raw films can be stretched by 10–15% in length. After the stretching, the tensile strength was improved from 180–198 to 500–600 MPa owing to the improved alignment. For the "wet" films which were infiltrated with 1 wt% BMI resin/acetone solutions, their strain at break were up to 20–25%, corresponding to the improved plasticity. This means that the impregnation prior to stretching also resulted in improved processability.

After the hot-pressing to cure BMI resins, the unstretched CNT/BMI films finally exhibited a tensile strength of 478–501 MPa. On the contrast, by first stretching the "wet" film by 20% and

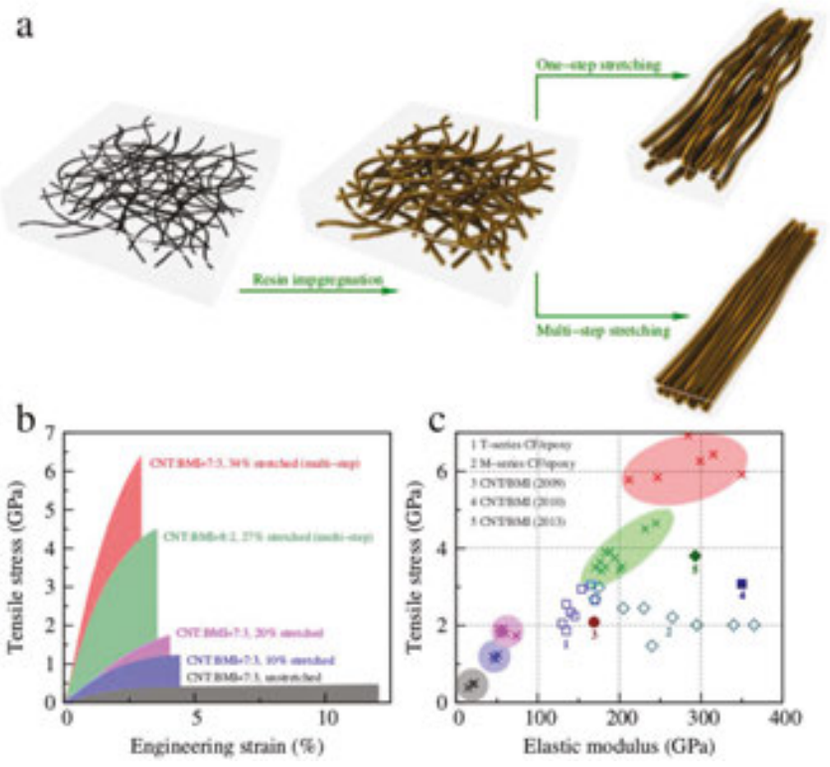

Figure 8. Bio-inspired aggregation control showed great advantages in realizing super-strong CNT composites [24]. (A) The schematic of preparation and stretching processes of CNT/polymer films. (B) The mechanical performances of CNT/BMI composite films under different stretching strategies. (C) A comparison of tensile strength and elastic modulus for CNT/BMI and carbon fiber/epoxy composites.

http://dx.doi.org/10.5772/62810

then curing the film, the strength increased up to 1.74–1.92 GPa. To further improve the mechanical properties, the stretching method was modified to a multi-step way (**Figure 8A**) and the "wet" films could be stretched by 27–34% after 8 to 10 steps. Notice that, in each step, 3% additional stretching, according to the immediate film length, was applied to the film, and there was always 5–10 min between steps to allow sufficient structure relaxation. After 8 or 10 steps, the total stretching magnitude was $1.03^8-1 = 0.267$ or $1.03^{10}-1 = 0.344$, respectively. In this multi-step way, the CNTs were fully aligned and the packing density during the hot-pressing was also improved. At this stage, the small-sized CNT bundles were well surrounded by the BMI resin molecules and maintained unaggregated phases. After being cured, the CNT/BMI composite films stably exhibited an extremely high tensile strength up to 4.5–6.94 GPa, depending on the CNT-to-resin mass ratio and the total stretching magnitude. At the same time, the elastic modulus was up to 232–315 GPa. Figure 8B shows the typical stress–strain curves for various CNT/BMI composite films, and Figure 8C provides the comparison with carbon fiber/epoxy composites.

5.3. Structural characterization

Based on the aggregation control and high CNT alignment, a big step has been realized towards the ideal composite structure. The tensile strength of >6 GPa is obviously much larger than those of carbon fiber/epoxy composites, in good agreement with their different composite structures (Figure 6). Figure 7D shows the cross-sectional picture of the CNT/BMI composite structure obtained by focused ion beam. Although individual CNTs were difficult to distinguish, CNT bundles with small size were found perpendicular to the cross section and their surfaces were all surrounded by BMI resins. Obviously, the maximized interface contacts can allow the most efficient interfacial stress transfer. Notice that the level of CNT aggregation was within 20–50 nm. This means that there is still a big challenge to obtain the ideal composite structure where individual CNTs are aligned, highly packed, and unaggregated.

5.4. Electrical properties

The ability to conduct electricity of a thin film is usually characterized by sheet resistance or square resistance, in units of "ohms per square". The square resistance of the as-produced CNT web was 1.194 $\Omega\ sq^{-1}$. After being impregnated with BMI resins, the resistance decreased to 0.926 $\Omega\ sq^{-1}$, as a result of the enhanced densification. After being stretched, the CNTs became aligned and the connection between CNT bundles were separated by the matrix. As a result, the resistance increased to 1.461 and 1.931 $\Omega\ sq^{-1}$ before and safer the curing process. The electrical conductivity of the final film was ~1700 S cm^{-1}, about 0.3 or 12% of copper's or stainless steel's electrical conductivity.

6. Conclusion

High-volume fraction CNT composites have exhibited exciting mechanical and electrical performances due to the high utilization of the CNT's intrinsic properties. The layer-by-layer stacking of aligned CNT sheets and the stretching of entangled CNT webs have provided two different solutions to realize the high-strength CNT composite films. Considering the easy

aggregation between CNTs, the bio-inspired aggregation control makes a big step to approach the ideal composite structure where the CNTs are highly packed, aligned, and unaggregated. The highest tensile strength of the CNT/BMI composite film can be up to 6.94 GPa, much higher than the strength of carbon fiber-reinforced polymers. We anticipate that the present fabrication method can be generalized for developing multifunctional and smart nanocomposites.

Acknowledgements

The authors thank financial supports from the National Natural Science Foundation of China (11302241, 11404371, 21273269, 21473238, 21503267, 51561145008) and the Youth Innovation Promotion Association of the Chinese Academy of Sciences (2015256, Grant to X.Z.).

Author details

Xiaohua Zhang*, Xueping Yu, Jingna Zhao and Qingwen Li

*Address all correspondence to: xhzhang2009@sinano.ac.cn

Key Laboratory of Nano-Devices Applications, Suzhou Institute of Nano-Tech Nano-Bionics, Chinese Academy of Sciences, Suzhou, China

References

[1] S. Iijima. Helical microtubules of graphitic carbon. Nature 354, 56 (1991).

[2] J. N. Coleman, U. Khan, W. J. Blau, and Y. K. Gun'ko. Small but strong: a review of the mechanical properties of carbon nanotube–polymer composites. Carbon 44, 1624 (2006).

[3] M. Moniruzzaman and K. I. Winey. Polymer nanocomposites containing carbon nanotubes. Macromolecules 39, 5194 (2006).

[4] P. M. Ajayan, O. Stephan, C. Colliex, and D. Trauth. Aligned carbon nanotube arrays formed by cutting a polymer resin–nanotube composite. Science 265, 1212 (1994).

[5] A. B. Dalton, S. Collins, E. Muñoz, J. M. Razal, V. H. Ebron, J. P. Ferraris, J. N. Coleman, B. G. Kim, and R. H. Baughman. Super-tough carbon-nanotube fibres. Nature 423, 703 (2003).

[6] C. Fang, J. Zhao, J. Jia, Z. Zhang, X. Zhang, and Q. Li. Enhanced carbon nanotube fibers by polyimide. Appl. Phys. Lett. 97, 181906 (2010).

[7] S. Li, X. Zhang, J. Zhao, F. Meng, G. Xu, Z. Yong, J. Jia, Z. Zhang, and Q. Li. Enhancement of carbon nanotube fibres using different solvents and polymers. Compos. Sci. Technol. 72, 1402 (2012).

[8] N. R. Raravikar, L. S. Schadler, A. Vijayaraghavan, Y. Zhao, B. Wei, and P. M. Ajayan. Synthesis and characterization of thickness-aligned carbon nanotube–polymer composite films. Chem. Mater. 17, 974 (2005).

[9] H. Cebeci, R. G. de Villoria, A. J. Hart, and B. L. Wardle. Multifunctional properties of high volume fraction aligned carbon nanotube polymer composites with controlled morphology. Compos. Sci. Technol. 69, 2649 (2009).

[10] T.-W. Chou, L. Gao, E. T. Thostenson, Z. Zhang, and J.-H. Byun. An assessment of the science and technology of carbon nanotube-based fibers and composites. Compos. Sci. Technol. 70, 1 (2010).

[11] P. D. Bradford, X. Wang, H. Zhao, J.-P. Maria, Q. Jia, and Y. T. Zhu. A novel approach to fabricate high volume fraction nanocomposites with long aligned carbon nanotubes. Compos. Sci. Technol. 70, 1980 (2010).

[12] W. Liu, X. Zhang, G. Xu, P. D. Bradford, X. Wang, H. Zhao, Y. Zhang, Q. Jia, F.-G. Yuan, Q. Li, Y. Qiu, and Y. Zhu. Producing superior composites by winding carbon nanotubes onto a mandrel under a poly(vinyl alcohol) spray. Carbon 49, 4786 (2011).

[13] J. N. Coleman, W. J. Blau, A. B. Dalton, E. Muñoz, S. Collins, B. G. Kim, J. Razal, M. Selvidge, G. Vieiro, and R. H. Baughman. Improving the mechanical properties of single-walled carbon nanotube sheets by intercalation of polymeric adhesives. Appl. Phys. Lett. 82, 1682 (2003).

[14] Z. Wang, Z. Liang, B. Wang, C. Zhang, and L. Kramer. Processing and property investigation of single-walled carbon nanotube (SWNT) buckypaper/epoxy resin matrix nanocomposites. Compos. Part A 35, 1225 (2004).

[15] P. Gonnet, Z. Liang, E. S. Choi, R. S. Kadambala, C. Zhang, J. S. Brooks, B. Wang, and L. Kramer. Thermal conductivity of magnetically aligned carbon nanotube buckypapers and nanocomposites. Curr. Appl. Phys. 6, 119 (2006).

[16] Z. Špitalský, C. Aggelopoulos, G. Tsoukleri, C. Tsakiroglou, J. Parthenios, S. Georga, C. Krontiras, D. Tasis, K. Papagelis, and C. Galiotis. The effect of oxidation treatment on the properties of multi-walled carbon nanotube thin films. Mater. Sci. Eng. B 165, 135 (2009).

[17] M. Zhang, S. Fang, A. A. Zakhidov, S. B. Lee, A. E. Aliev, C. D. Williams, K. R. Atkinson, and R. H. Baughman. Strong, transparent, multifunctional, carbon nanotube sheets. Science 309, 1215 (2005).

[18] Y.-L. Li, I. A. Kinloch, and A. H. Windle. Direct spinning of carbon nanotube fibers from chemical vapor deposition synthesis. Science 304, 276 (2004).

[19] T. L. B. Ha, T. M. Quan, D. N. Vu, and D. M. Si. Naturally derived biomaterials: preparation and application. "Regenerative Medicine and Tissue Engineering" (Edited by J. A. Andrades, InTech - Open Access, Rijeka, Croatia, 2013) Chapter 11, pp. 247–274.

[20] T. Giesa, M. Arslan, N. M. Pugno, and M. J. Buehler. Nanoconfinement of spider silk fibrils begets superior strength, extensibility, and toughness. Nano Lett. 11, 5038 (2011).

[21] C. M. Preston and B. G. Sayer. What's in a nutshell: an investigation of structure by carbon-13 cross-polarization magic-angle spinning nuclear magnetic resonance spectroscopy. J. Agric. Food Chem. 40, 206 (1992).

[22] S. M. Porter. Seawater chemistry and early carbonate biomineralization. Science 316, 1302 (2007).

[23] Q. Cheng, L. Jiang, and Z. Tang. Bioinspired layered materials with superior mechanical performance. Acc. Chem. Res. 47, 1256 (2014).

[24] Y. Han, X. Zhang, X. Yu, J. Zhao, S. Li, F. Liu, P. Gao, Y. Zhang, T. Zhao, and Q. Li. Bioinspired aggregation control of carbon nanotubes for ultra-strong composites. Sci. Rep. 5, 11533 (2015).

[25] J. N. Coleman, U. Khan, and Y. K. Gun'ko. Mechanical reinforcement of polymers using carbon nanotubes. Adv. Mater. 18, 689 (2006).

[26] B. Fiedler, F. H. Gojny, M. H. G. Wichmann, M. C. M. Nolte, and K. Schulte. Fundamental aspects of nano-reinforced composites. Compos. Sci. Technol. 66, 3115 (2006).

[27] X.-L. Xie, Y.-W. Mai, and X.-P. Zhou. Dispersion and alignment of carbon nanotubes in polymer matrix: a review. Mater. Sci. Eng. R 49, 89 (2005).

[28] Z. Spitalsky, D. Tasis, K. Papagelis, and C. Galiotis. Carbon nanotube–polymer composites: chemistry, processing, mechanical and electrical properties. Prog. Polym. Sci. 35, 357 (2010).

[29] M. Rahmat and P. Hubert. Carbon nanotube–polymer interactions in nanocomposites: a review. Compos. Sci. Technol. 72, 72 (2011).

[30] L. Jin, C. Bower, and O. Zhou. Alignment of carbon nanotubes in a polymer matrix by mechanical stretching. Appl. Phys. Lett. 73, 1197 (1998).

[31] M. S. P. Shaffer and A. H. Windle. Fabrication and characterization of carbon nanotube/poly(vinyl alcohol) composites. Adv. Mater. 11, 937 (1999).

[32] X. Gong, J. Liu, S. Baskaran, R. D. Voise, and J. S. Young. Surfactant-assisted processing of carbon nanotube/polymer composites. Chem. Mater. 12, 1049 (2000).

[33] A. Dufresne, M. Paillet, J. Putaux, R. Canet, F. Carmona, P. Delhaes, and S. Cui. Processing and characterization of carbon nanotube/poly (styrene-co-butyl acrylate) nanocomposites. J. Mater. Sci. 37, 3915 (2002).

[34] O. Probst, E. M. Moore, D. E. Resasco, and B. P. Grady. Nucleation of polyvinyl alcohol crystallization by single-walled carbon nanotubes. Polymer 45, 4437 (2004).

[35] F. Dalmas, L. Chazeau, C. Gauthier, K. Masenelli-Varlot, R. Dendievel, J.-Y. Cavaille, and L. Forro. Multiwalled carbon nanotube/polymer nanocomposites: processing and properties. J. Polym. Sci. B: Polym. Phys. 43, 1186 (2005).

[36] M. Zhang, L. Su, and L. Mao. Surfactant functionalization of carbon nanotubes (CNTs) for layer-by-layer assembling of CNT multi-layer films and fabrication of gold nanoparticle/CNT nanohybrid. Carbon 44, 276 (2006).

[37] S. Bose, R. A. Khare, and P. Moldenaers. Assessing the strengths and weaknesses of various types of pre-treatments of carbon nanotubes on the properties of polymer/carbon nanotubes composites: a critical review. Polymer 51, 975 (2010).

[38] Y. Y. Huang and E. M. Terentjev. Dispersion of carbon nanotubes: mixing, sonication, stabilization, and composite properties. Polymers 4, 275 (2012).

[39] P. Pötschke, A. R. Bhattacharyya, A. Janke, and H. Goering. Melt mixing of polycarbonate/multi-wall carbon nanotube composites. Compos. Interfaces 10, 389 (2003).

[40] O. Breuer and U. Sundararaj. Big returns from small fibers: a review of polymer/carbon nanotube composites. Polym. Compos. 25, 630 (2004).

[41] E. J. Siochi, D. C. Working, C. Park, P. T. Lillehei, J. H. Rouse, C. C. Topping, A. R. Bhattacharyya, and S. Kumar. Melt processing of SWCNT–polyimide nanocomposite fibers. Compos. Part B 35, 439 (2004).

[42] W. D. Zhang, L. Shen, I. Y. Phang, and T. Liu. Carbon nanotubes reinforced nylon-6 composite prepared by simple melt-compounding. Macromolecules 37, 256 (2004).

[43] B. Lin, U. Sundararaj, and P. Pötschke. Melt mixing of polycarbonate with multi-walled carbon nanotubes in miniature mixers. Macromol. Mater. Eng. 291, 227 (2006).

[44] Z. Jia, Z. Wang, C. Xu, J. Liang, B. Wei, D. Wu, and S. Zhu. Study on poly (methyl methacrylate)/carbon nanotube composites. Mater. Sci. Eng. A 271, 395 (1999).

[45] C. Velasco-Santos, A. L. Martínez-Hernández, F. T. Fisher, R. Ruoff, and V. M. Castano. Improvement of thermal and mechanical properties of carbon nanotube composites through chemical functionalization. Chem. Mater. 15, 4470 (2003).

[46] K. W. Putz, C. A. Mitchell, R. Krishnamoorti, and P. F. Green. Elastic modulus of single-walled carbon nanotube/poly (methyl methacrylate) nanocomposites. J. Polym. Sci. B: Polym. Phys. 42, 2286 (2004).

[47] S. Kumar, T. D. Dang, F. E. Arnold, A. R. Bhattacharyya, B. G. Min, X. Zhang, R. A. Vaia, C. Park, W. W. Adams, R. H. Hauge, R. E. Smalley, S. Ramesh, and P. A. Willis. Synthesis, structure, and properties of PBO/SWNT composites. Macromolecules 35, 9039 (2002).

[48] C. Zhao, G. Hu, R. Justice, D. W. Schaefer, S. Zhang, M. Yang, and C. C. Han. Synthesis and characterization of multi-walled carbon nanotubes reinforced polyamide 6 via in situ polymerization. Polymer 46, 5125 (2005).

[49] Y. Lin, B. Zhou, K. A. S. Fernando, P. Liu, L. F. Allard, and Y.-P. Sun. Polymeric carbon nanocomposites from carbon nanotubes functionalized with matrix polymer. Macromolecules 36, 7199 (2003).

[50] C. A. Dyke and J. M. Tour. Covalent functionalization of single-walled carbon nanotubes for materials applications. J. Phys. Chem. A 108, 11151 (2004).

[51] K. Balasubramanian and M. Burghard. Chemically functionalized carbon nanotubes. Small 1, 180 (2005).

[52] L. Xie, F. Xu, F. Qiu, H. Lu, and Y. Yang. Single-walled carbon nanotubes functionalized with high bonding density of polymer layers and enhanced mechanical properties of composites. Macromolecules 40, 3296 (2007).

[53] C. Bartholome, P. Miaudet, A. Derré, M. Maugey, O. Roubeau, C. Zakri, and P. Poulin. Influence of surface functionalization on the thermal and electrical properties of nanotube–PVA composites. Compos. Sci. Technol. 68, 2568 (2008).

[54] Y. Hou, J. Tang, H. Zhang, C. Qian, Y. Feng, and J. Liu. Functionalized few-walled carbon nanotubes for mechanical reinforcement of polymeric composites. ACS Nano 3, 1057 (2009).

[55] P.-C. Ma, N. A. Siddiqui, G. Marom, and J.-K. Kim. Dispersion and functionalization of carbon nanotubes for polymer-based nanocomposites: a review. Compos. Part A 41, 1345 (2010).

[56] H. Xia, Q. Wang, and G. Qiu. Polymer-encapsulated carbon nanotubes prepared through ultrasonically initiated in situ emulsion polymerization. Chem. Mater. 15, 3879 (2003).

[57] S. Qin, D. Qin, W. T. Ford, D. E. Resasco, and J. E. Herrera. Functionalization of single-walled carbon nanotubes with polystyrene via grafting to and grafting from methods. Macromolecules 37, 752 (2004).

[58] G. L. Hwang, Y.-T. Shieh, and K. C. Hwang. Efficient load transfer to polymer-grafted multiwalled carbon nanotubes in polymer composites. Adv. Funct. Mater. 14, 487 (2004).

[59] H.-J. Jin, H. J. Choi, S. H. Yoon, S. J. Myung, and S. E. Shim. Carbon nanotube-adsorbed polystyrene and poly (methyl methacrylate) microspheres. Chem. Mater. 17, 4034 (2005).

[60] M. Salami-Kalajahi, V. Haddadi-Asl, F. Behboodi-Sadabad, S. Rahimi-Razin, and H. Roghani-Mamaqani. Properties of PMMA/carbon nanotubes nanocomposites prepared by "grafting through" method. Polym. Compos. 33, 215 (2012).

[61] X. Tong, C. Liu, H.-M. Cheng, H. Zhao, F. Yang, and X. Zhang. Surface modification of single-walled carbon nanotubes with polyethylene via in situ Ziegler-Natta polymerization. J. Appl. Polym. Sci. 92, 3697 (2004).

[62] M. L. Shofner, V. N. Khabashesku, and E. V. Barrera. Processing and mechanical properties of fluorinated single-wall carbon nanotube–polyethylene composites. Chem. Mater. 18, 906 (2006).

[63] B.-X. Yang, K. P. Pramoda, G. Q. Xu, and S. H. Goh. Mechanical reinforcement of polyethylene using polyethylene-grafted multiwalled carbon nanotubes. Adv. Funct. Mater. 17, 2062 (2007).

[64] J. F. Vega, Y. da Silva, E. Vicente-Alique, R. Núñez-Ramírez, M. Trujillo, M. L. Arnal, A. J. Müller, P. Dubois, and J. Martínez-Salazar. Influence of chain branching and molecular weight on melt rheology and crystallization of polyethylene/carbon nanotube nanocomposites. Macromolecules 47, 5668 (2014).

[65] H. Li, F. Cheng, A. M. Duft, and A. Adronov. Functionalization of single-walled carbon nanotubes with well-defined polystyrene by "click" coupling. J. Am. Chem. Soc. 127, 14518 (2005).

[66] B. Fragneaud, K. Masenelli-Varlot, A. Gonzalez-Montiel, M. Terrones, and J.-Y. Cavaillé. Mechanical behavior of polystyrene grafted carbon nanotubes/polystyrene nanocomposites. Compos. Sci. Technol. 68, 3265 (2008).

[67] B. P. Grady, A. Paul, J. E. Peters, and W. T. Ford. Glass transition behavior of single-walled carbon nanotube–polystyrene composites. Macromolecules 42, 6152 (2009).

[68] Z. Wu, W. Feng, Y. Feng, Q. Liu, X. Xu, T. Sekino, A. Fujii, and M. Ozaki. Preparation and characterization of chitosan-grafted multiwalled carbon nanotubes and their electrochemical properties. Carbon 45, 1212 (2007).

[69] J. Venkatesan, Z.-J. Qian, B. Ryu, N. A. Kumar, and S.-K. Kim. Preparation and characterization of carbon nanotube-grafted-chitosan–natural hydroxyapatite composite for bone tissue engineering. Carbohydr. Polym. 83, 569 (2011).

[70] J. N. Coleman, M. Cadek, R. Blake, V. Nicolosi, K. P. Ryan, C. Belton, A. Fonseca, J. B. Nagy, Y. K. Gun'ko, and W. J. Blau. High performance nanotube-reinforced plastics: understanding the mechanism of strength increase. Adv. Funct. Mater. 14, 791 (2004).

[71] H. Deng, R. Zhang, C. T. Reynolds, E. Bilotti, and T. Peijs. A novel concept for highly oriented carbon nanotube composite tapes or fibres with high strength and electrical conductivity. Macromol. Mater. Eng. 294, 749 (2009).

[72] B. S. Shim, J. Zhu, E. Jan, K. Critchley, S. Ho, P. Podsiadlo, K. Sun, and N. A. Kotov. Multiparameter structural optimization of single-walled carbon nanotube composites: toward record strength, stiffness, and toughness. ACS Nano 3, 1711 (2009).

[73] Y. Wang, F. Wei, G. Luo, H. Yu, and G. Gu. The large-scale production of carbon nanotubes in a nano-agglomerate fluidized-bed reactor. Chem. Phys. Lett. 364, 568 (2002).

[74] Q. Zhang, J.-Q. Huang, M.-Q. Zhao, W.-Z. Qian, and F. Wei. Carbon nanotube mass production: principles and processes. ChemSusChem 4, 864 (2011).

[75] K. Jiang, Q. Li, and S. Fan. Spinning continuous carbon nanotube yarns. Nature 419, 801 (2002).

[76] M. Zhang, K. R. Atkinson, and R. H. Baughman. Multifunctional carbon nanotube yarns by downsizing an ancient technology. Science 306, 1358 (2004).

[77] X. Zhang, K. Jiang, C. Feng, P. Liu, L. Zhang, J. Kong, T. Zhang, Q. Li, and S. Fan. Spinning and processing continuous yarns from 4-inch wafer scale super-aligned carbon nanotube arrays. Adv. Mater. 18, 1505 (2006).

[78] Q. Li, X. Zhang, R. F. DePaula, L. Zheng, Y. Zhao, L. Stan, T. G. Holesinger, P. N. Arendt, D. E. Peterson, and Y. T. Zhu. Sustained growth of ultralong carbon nanotube arrays for fiber spinning. Adv. Mater. 18, 3160 (2006).

[79] K. Liu, Y. Sun, L. Chen, C. Feng, X. Feng, K. Jiang, Y. Zhao, and S. Fan. Controlled growth of super-aligned carbon nanotube arrays for spinning continuous unidirectional sheets with tunable physical properties. Nano Lett. 8, 700 (2008).

[80] L. Zheng, G. Sun, and Z. Zhan. Tuning array morphology for high-strength carbon-nanotube fibers. Small 6, 132 (2010).

[81] Q. F. Cheng, J. P. Wang, J. J. Wen, C. H. Liu, K. L. Jiang, Q. Q. Li, and S. S. Fan. Carbon nanotube/epoxy composites fabricated by resin transfer molding. Carbon 48, 260 (2010).

[82] X. Wang, Z. Z. Yong, Q. W. Li, P. D. Bradford, W. Liu, D. S. Tucker, W. Cai, H. Wang, F. G. Yuan, and Y. T. Zhu. Ultrastrong, stiff and multifunctional carbon nanotube composites. Mater. Res. Lett. 1, 19 (2013).

[83] X. Wang, Q. Jiang, W. Xu, W. Cai, Y. Inoue, and Y. Zhu. Effect of carbon nanotube length on thermal, electrical and mechanical properties of CNT/bismaleimide composites. Carbon 53, 145 (2013).

[84] Y.-N. Liu, M. Li, Y. Gu, K. Wang, D. Hu, Q. Li, and Z. Zhang. A modified spray-winding approach to enhance the tensile performance of array-based carbon nanotube composite films. Carbon 65, 187 (2013).

[85] Q. Jiang, X. Wang, Y. Zhu, D. Hui, and Y. Qiu. Mechanical, electrical and thermal properties of aligned carbon nanotube/polyimide composites. Compos. Part B 56, 408 (2014).

[86] M. D. Frogley, Q. Zhao, and H. D. Wagner. Polarized resonance Raman spectroscopy of single-wall carbon nanotubes within a polymer under strain. Phys. Rev. B 65, 113413 (2002).

[87] J. Di, D. Hu, H. Chen, Z. Yong, M. Chen, Z. Feng, Y. Zhu, and Q. Li. Ultrastrong, foldable, and highly conductive carbon nanotube film. ACS Nano 6, 5457 (2012).

[88] Y. Wang, M. Li, Y. Gu, X. Zhang, S. Wang, Q. Li, and Z. Z. Zhang. Tuning carbon nanotube assembly for flexible, strong and conductive films. Nanoscale 7, 3060 (2015).

[89] L. Zhang, X. Wang, W. Xu, Y. Zhang, Q. Li, P. D. Bradford, and Y. Zhu. Strong and conductive dry carbon nanotube films by microcombing. Small 11, 3830 (2015).

[90] X. Yu, J. Zou, Z. Lan, C. Jiang, J. Zhao, D. Zhang, X. Zhang, M. Miao, and Q. Li. Solvent-tunable microstructures of aligned carbon nanotube films. (Unpulished results).

[91] J. Jia, J. Zhao, G. Xu, J. Di, Z. Yong, Y. Tao, C. Fang, Z. Zhang, X. Zhang, L. Zheng, and Q. Li. A comparison of the mechanical properties of fibers spun from different carbon nanotubes. Carbon 49, 1333 (2011).

[92] D. Lashmore, Supercapacitors and methods of manufacturing same, (2008), US Patent No. 20080225464.

[93] Q. Cheng, J. Bao, J. Park, Z. Liang, C. Zhang, and B. Wang. High mechanical performance composite conductor: multi-walled carbon nanotube sheet/bismaleimide nanocomposites. Adv. Funct. Mater. 19, 3219 (2009).

[94] J. E. Fischer, W. Zhou, J. Vavro, M. C. Llaguno, C. Guthy, R. Haggenmueller, M. J. Casavant, D. E. Walters, and R. E. Smalley. Magnetically aligned single wall carbon nanotube films: preferred orientation and anisotropic transport properties. J. Appl. Phys. 93, 2157 (2003).

[95] Q. Cheng, B. Wang, C. Zhang, and Z. Liang. Functionalized carbon-nanotube sheet/bismaleimide nanocomposites: mechanical and electrical performance beyond carbon-fiber composites. Small 6, 763 (2010).

[96] D. Gagnebien, P. J. Madec, and E. Maréchal. Synthesis of poly(sulphone-*b*-siloxane)s—I. Model study of the epoxy-phenol reaction in the melt. Eur. Polym. J. 21, 273 (1985).

[97] G. Wei and H. J. Sue. Fracture mechanisms in preformed polyphenylene oxide particle-modified bismaleimide resins. J. Appl. Polym. Sci. 74, 2539 (1999).

[98] Y. Li, J. Miranda, and H.-J. Sue. Hygrothermal diffusion behavior in bismaleimide resin. Polymer 42, 7791 (2001).

[99] H.D. Wagner. Nanocomposites: paving the way to stronger materials. Nat. Nanotechnol. 2, 742 (2007).

IntechOpen